The piezoelectric activity in the HfO_2 nanoclusters

Balabai R.M, Zadorozhnii V.M. *E-mail:balabai@i.ua, vitaliy_zadorozhniy@ukr.net*

Kryvyi Rih State Pedagogical University, 54 Gagarina Ave., Kryvyi Rih, 50086, Ukraine.

Introduction

Piezoelectric materials generate electric charge in response to physical stresses (the direct piezoelectric effect) or through deformation under an electric field (the inverse piezoelectric effect). These phenomena are related to the development of piezoresponse force microscopy, sensors, actuators, resonators, electric energy harvesters [1, 2]. It is important to know whether the signs of the piezoelectric coefficient in piezoelectric materials have uniform positive or negative values, or a mixture of local negative and positive responses. For example, it has been recently predicted from first principles that the usual ferroelectric phase of HfO_2 (orthorhombic with space group $Pca2_1$) presents a negative longitudinal piezoresponse. Though, existing experimental measurements of hafnia's piezoresponse suggest a perovskite-like behavior (i.e., a positive longitudinal effect) [3]. Research at the atomic level is needed to elucidate the physical mechanisms governing these phenomena.

In this paper the piezoelectric effects of the HfO_2 nanofilms are studied by methods of the density functional theory and first-principles pseudopotential based on own program code [4]. The spatial distribution of valence electron density, density of states, and Coulomb potential along transverse direction are calculated. Local force responses from the electronic subsystem, cationic, anionic sublattices of hafnium oxide to multidirectional deformations are discussed.

Research methods and models

All calculations have been made with the proprietary source code [4]. The basic states of the electron-nucleus systems were detected by means of the self-consistent solution of Kohn-Sham one-particle equations:

$$\left\{-\frac{h^2}{2m}\nabla^2+\frac{\partial U}{\partial n(\mathbf{r})}\right\}\psi_i(\mathbf{r})=\varepsilon_i\psi_i(\mathbf{r}) \qquad (1)$$

In the solution of these equations, the pseudopotential formalism was used, according to which a solid is considered as a set of valence electrons and the ion cores. In the pseudopotential approximation, the operator of the pseudopotential V_{PS}, which describes the interaction of valence electrons with the core, is small, and the corresponding pseudo-wavefunction is smooth. Bachelet-Hamann- Schliiter *ab initio* pseudopotential is used by us. The full crystalline potential is constructed as the sum of ion pseudopotentials that are not overlapping and associated with ions (nucleus + core electrons), located at the $\vec{R}_S$ positions that are periodically repeated for crystals:

$$V_{crystal}(\vec{r}) \to V_{PS}(\vec{r}) = \sum_{\vec{p}}\sum_{S} \hat{V}_S^{PS}(\vec{r}-\vec{p}-\vec{R}_S) \qquad (2)$$

For nonperiodic systems, such as a thin film or a cluster the problem of lack of periodicity is circumvented by use of the supercell method. Namely, the cluster is periodically repeated but the distance between each cluster and its periodic images is so large that their interaction is negligible. The ubiquitous periodicity of the crystal (or artificial) lattice produces a periodic potential and thus imposes the same periodicity on the density (implying Bloch's Theorem). The Kohn-Sham potential of a periodic system exhibits the same periodicity as the direct lattice and the Kohn-Sham orbitals can be written in Bloch form:

$$\psi(\vec{r}) = \psi_i(\vec{r},\vec{k}) = exp(i\vec{k}\cdot\vec{r})u_i(\vec{r},\vec{k}) \qquad (3)$$

where $\vec{k}$ is a vector in the first Brillouin zone. The functions $u_i(\vec{r},\vec{k})$ have the periodicity of the direct lattice. The index «*i*» runs over all states. The periodic functions $u_i(\vec{r},\vec{k})$ are expanded in the plane wave basis. This heavily suggests using plane waves as the generic basis set in order to expand the periodic part of the orbitals. Since plane waves form a complete and orthonormal set of functions, they can be used to expand orbitals according to:

$$\Psi_j(\vec{k},\vec{r}) = \frac{1}{\sqrt{N_0}\sqrt{\Omega}}\sum_{\vec{G}} b_j(\vec{k}+\vec{G})\ exp(i(\vec{k}+\vec{G})\vec{r}) \qquad (4)$$

where $\vec{G}$ is the vector in the reciprocal space, Ω is the volume of the elemental cells which consists of a periodic crystal or an artificial superlattice when reproducing nonperiodic objects.

The equation (1) after the Fourier transform to the reciprocal space has the form:

$$\sum_{\vec{G}}\left[\left\{\frac{\hbar^2}{2m}(\vec{k}+\vec{G})^2-\varepsilon_j\right\}\delta_{\vec{G},\vec{G}'}+V_{KS}(\vec{k}+\vec{G},\vec{k}+\vec{G}')\right]b_j(\vec{k}+\vec{G})=0 \qquad (5)$$

where V_{KS} is the Kohn-Sham potential:

$$V_{KS}(\vec{k}+\vec{G},\vec{k}+\vec{G}') = V_{ps}(\vec{k}+\vec{G},\vec{k}+\vec{G}') + V_H(\vec{G}'-\vec{G}) + V_{XC}(\vec{G}'-\vec{G}) \qquad (6)$$

where V_{xc} is the the exchange and correlation potential. To calculate its we used Ceperley-Alder's approximation that has been parameterized by Perdew and Zunger.

The main value in the formalism of the functional of the electron density is the charge density. It is estimated from a self-consistent solution of equations (1) which should be performed at all points of the non-reduced section of the Brillouin zone:

$$\rho(\mathbf{G}) = \frac{2}{N_T}\sum_{\mathbf{k}}\sum_{\mathbf{j}}\sum_{\alpha\in T}\sum_{\mathbf{G}} b_j^*(\mathbf{k}+\mathbf{G}'+\alpha\mathbf{G})b_j(\mathbf{k}+\mathbf{G}') \qquad (7)$$

where the index *j* runs over all occupied states, $\vec{k}$ is a vector in the first Brillouin zone, N_T is the number of the operators α in the point group T of the atomic basis and the factor 2 takes into account the spin degeneracy.

Coulomb potential along the given direction was calculated by the formula that in the reciprocal space has the form:

$$V_h(\mathbf{G}) = \frac{4\pi e^2\rho(\mathbf{G})}{G^2} \qquad (8)$$

where $\rho(\mathbf{G})$ is the Fourier component of the electron density (7).

Our calculations were made under the following conditions: the Brillouin zone (ZB) summation was changed by calculation at one point of the ZB (Γ-point). The self-consistency iterations were terminated if the results of the current iteration calculation coincided with the previous one with a predetermined error. Usually, our results coincided after 5-6 iterations. The number of plane waves was chosen to be about 20-25 waves per base atom. The atomic basis was not optimized.

The force acting on atom *s* is the negative derivative of the total energy with respect to a basis vector $\boldsymbol{\tau}_s$. The terms containing implicit derivatives of the wave functions vanish according to Hellmann-Feynman theorem. Therefore, the calculation of forces is performed by a formula:

$$\mathbf{F}^s = \mathbf{F}_e^s + \mathbf{F}_c^s \qquad (9)$$

where components of electronic and ionic interactions are defined:

$$\mathbf{F}_e^s = i\Omega_c\sum_{\mathbf{G}}\rho^*(\mathbf{G})\mathbf{G}e^{-i\mathbf{G}\boldsymbol{\tau}_s}v_s(\mathbf{G}) - \\ -\sum_{i,\mathbf{G},\mathbf{G}',l} n_i\Psi_i^*(\mathbf{k}_i+\mathbf{G}')\Psi_i(\mathbf{k}_i+\mathbf{G})(\mathbf{G}-\mathbf{G}')e^{-i(\mathbf{G}-\mathbf{G}')\boldsymbol{\tau}_s}v'_{s,l}(\mathbf{k}_i+\mathbf{G},\mathbf{k}_i+\mathbf{G}'), \qquad (10)$$

$$\mathbf{F}_c^s = 2Z_s\sum_{s'\neq s}Z_{s'}\frac{4\pi}{\Omega_c}\sum_{\mathbf{G}}{}'\left(\frac{\mathbf{G}}{|\mathbf{G}|^2}sin\left(\mathbf{G}(\mathbf{T}_s-\boldsymbol{\tau}_{s'})\right)e^{-\frac{|\mathbf{G}|^2}{4\eta^2}}\right) + \\ +2Z_s\sum_{s'\neq s}Z_{s'}\sum_{\mathbf{l}}\left(\frac{\mathbf{x}\,erfc(\eta|\mathbf{x}|)}{|\mathbf{x}|^3}+\frac{2\eta\mathbf{x}}{\sqrt{\pi}|\mathbf{x}|^2}e^{-|\mathbf{x}|^2}\right). \qquad (11)$$

There are $\mathbf{x}=\mathbf{l}+\boldsymbol{\tau}_s-\boldsymbol{\tau}_{s'}$, Ω_c – atom volume, $\boldsymbol{\tau}_s$ – basic vector of atom *s*, Z_s – core's charge, l – lattice vector, η – parameter of the convergence of the amount in the Ewald's function *erfc*.

For calculations such object was developed: the infinite free-standing film with six mono-layers of non centro-symmetric orthorhombic HfO_2 with the space group of $Pca2_1$. This phase is widely recognized as the most responsible for ferroelectricity behavior [5]. The $Pca2_1$ bulk has an orthorhombic structure with twelve atoms per primitive unit cell. Multiplicity, Wyckoff letter, fractional coordinates for Hf and O atoms are 4a;

(1) x , y , z ; (2) ¯x , ¯y , z + ½; (3) x + ½ , ¯y , z; (4) ¯x + ½, y , z + ½;

Hf1: x=0.0337a; y=0.2670b; z=0.4989c;

O1: x=0.3654a; y=0.0701b; z=0.6444c;

O2: x= 0.7320a; y=0.4511b; z=0.7498c;

a=5.291 Å, b=5.063 Å, c=5.093 Å.

The single cell of the super-lattice was with parameters a=5.291 Å, b=5.063 Å, c=10 Å; the base consisted of 12 atoms (four of Hf atoms and eight of O atoms). The unit cell of the crystal and the unit cell of the superlattice had the same parameters in the ***a*** and ***b*** crystallographic directions, which are conjugated with the X and Y axes, and different in the ***c*** (Z) direction. Such values of the parameters of a single superlattice cell simulated an infinite film in the X, Y direction and a finite (100) film thickness of 4.54 angstroms in the Z direction, due to the introduction of vacuum layers into the cell, as in Fig. 1.

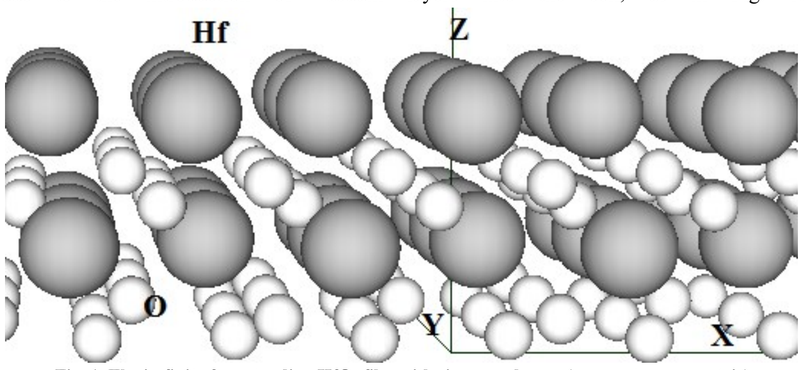

Fig. 1. The in finite free-standing HfO_2 film with six mono-layers (non centro-symmetric)

Modeling of mechanical effects of the static compression type was carried out by changing the corresponding coordinates of atoms in the direction of the compression force: for a film with free surfaces (001), the compression force acted in the [001] direction, which is conjugate to the Cartesian direction Z, and, accordingly, Z-coordinates of atoms decreased up to 20% of the original with a step of 3%.

Result and discussion

The results of the analysis of changes in the distribution of valence electrons in the area of the films, forces that act on an individual atom from the electronic and ionic subsystems of the film, the reliefs of the distribution of the Coulomb potential across atomic layers of film under the influence of mechanical compression of the film are shown in tables and figures.

For individual crystals of materials with an ionic component of a chemical bond with a structure devoid of central symmetry, there is a certain type of surface orientations called polar surfaces. A formal definition for these surfaces can be obtained by considering the projection of the dipole moment associated with the unit cell (which is nonzero because there is no central symmetry) onto the normal to the surface. If this projection is non-zero for a given surface orientation, the term "polar surface" is used. In the case of HfO_2, the dipole moment of the unit cell is directed along the [001] crystallographic direction. The presence of a non-zero dipole moment per unit cell for polar surfaces leads to the appearance of an electrostatic field. Analyzing the changes in the distribution of electric potentials in the area of surfaces, it is possible to estimate the degree of influence of mechanical compression on the general distribution of electron density, because it determines the potential distribution. The transition of the electronic charge from the surface lined with hafnium atoms to the opposite surface lined with oxygen atoms is observed for compressed films.

On the maps of the spatial distribution of the density of valence electrons in the film, a sharp polarization is recorded, namely, the electron charge is grouped on the oxygen surface of the film, leaving the positively charged ionic cores of hafnium on the opposite surface of the film unshielded. Such a charge distribution of valence electrons is fixed in the film without mechanical action; in the presence of compression, the polarization in the charge distribution becomes more intense (Fig. 1).

On Fig. 2 shows the cross section of the spatial charge distribution of valence electrons, which captures most of the infinite film. This figure shows changes in the form of charge transfer from hafnium atoms to oxygen atoms.

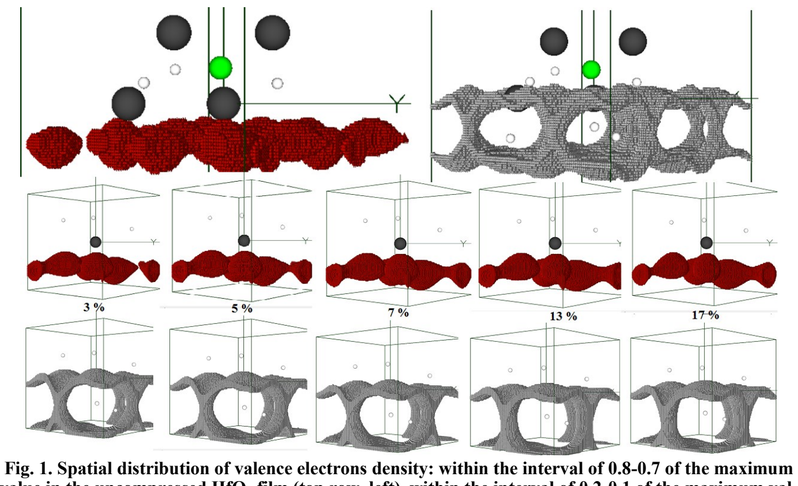

Fig. 1. Spatial distribution of valence electrons density: within the interval of 0.8-0.7 of the maximum value in the uncompressed HfO_2 film (top row, left), within the interval of 0.2-0.1 of the maximum value in the uncompressed HfO_2 film (top row, right). The middle and bottom rows show the same distributions in compressed film

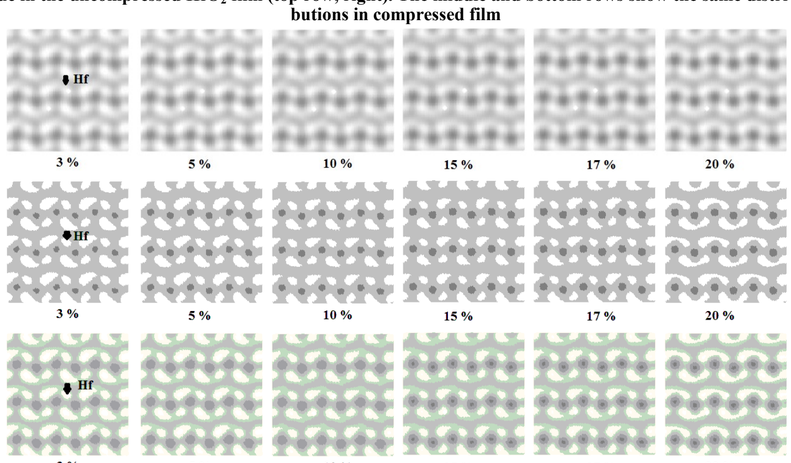

Fig. 2. Cross-sections of the spatial distributions of the valence electron density in an infinite HfO_2 film with the (001) free surfaces at various mechanical compression levels of the film from 3 to 20%. (Various graphic file formats are given to be able to catch the differences)

The electron charge from the oxygen surface is pushed out of the film with an increase in the level of its compression. This effect is visible in Fig. 3, which shows the electron density distribution at the oxygen surfaces of two closely spaced films. Figure 3 shows the absence of electron density in the interfilm space upon compression of the films to 17% and the filling of this space upon compression to 20%, while the distance between the films did not decrease.

Whereas on the maps of the spatial distribution of the density of valence electrons in the cluster, the charge polarization is not fixed (Fig. 4). The cluster contained 12 atoms. On Fig. 3 shows the same region of space as for the film. Cluster compression did not lead to polar charge redistribution.

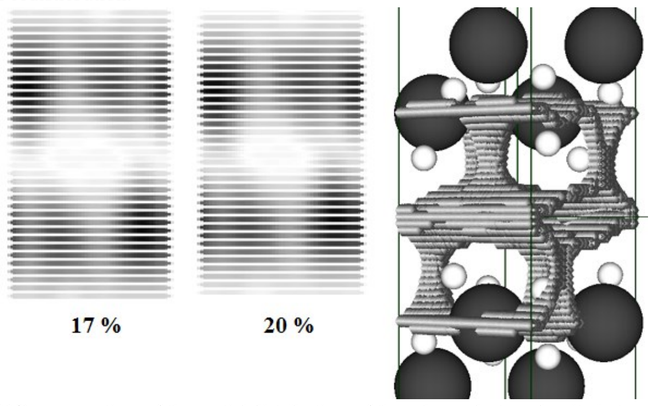

Fig. 3. (110) cross-sections of the spatial distributions of the valence electron density in two infinite HfO_2 films with the (001) free surfaces at various mechanical compression levels of the film from 17 to 20% (left); spatial distribution of valence electrons density within the interval of 0.2-0.1 of the maximum value in the 20 % compressed HfO_2 films (right)

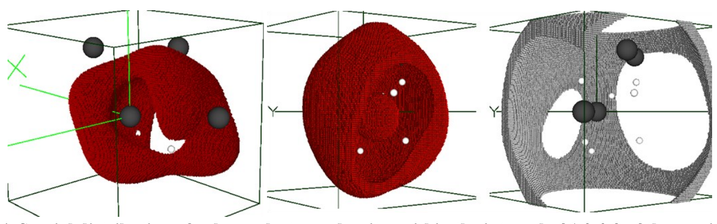

Fig. 4. Spatial distribution of valence electrons density: within the interval of 1.0-0.9 of the maximum value in the uncompressed HfO_2 cluster (left), within the interval of 0.8-0.7 of the maximum value in the uncompressed HfO_2 cluster (middle), within the interval of 0.2-0.1 of the maximum value in the uncompressed HfO_2 cluster (right)

Table 1 contains reliefs of distributions of electric potentials calculated by formula 8 along the lines in different layers of the film, which are indicated in Fig. 5.

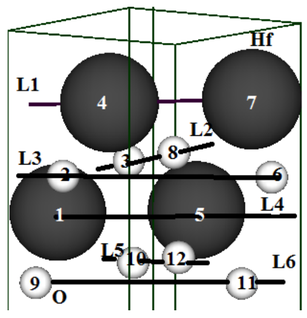

Fig. 5. The numbering of atoms, atomic layers correspond to the numbering in tables 1-3. A single cell with an atomic basis is shown; translation of single cell models an infinite film in the X Y plane

Table 1. Distributions of electric potentials along different layers of the HfO_2 film

%	Hf Layer 4 (external) Atoms1-5	Hf Layer 1 (inside) Atoms4-7	O Layer 3 (inside) Atoms2-6	O Layer 2 (inside) Atoms3-8	O Layer 6 (external) Atoms9-11	O Layer 5 (external) Atoms10-12
0	U_{max}=7,901 U_{min}=7,416	U_{max}=-10,841 U_{min}=-10,871	U_{max}=1,424 U_{min}=1,240	U_{max}=-2,670 U_{min}=-2,732	U_{max}=19,024 U_{min}=17,924	U_{max}=17,212 U_{min}=16,038
5	U_{max}=9,010 U_{min}=8,529	U_{max}=-9,907 U_{min}=-9,937	U_{max}=2,518 U_{min}=2,301	U_{max}=-1,566 U_{min}=-1,637	U_{max}=20,771 U_{min}=19,510	U_{max}=18,847 U_{min}=17,279
10	U_{max}=10,228 U_{min}=9,772	U_{max}=-8,708 U_{min}=	U_{max}=3,755 U_{min}=3,545	U_{max}=-0,323 U_{min}=-0,397	U_{max}=22,518 U_{min}=21,272	U_{max}=19,860 U_{min}=18,684
15	U_{max}=11,629 U_{min}=11,178	U_{max}=-7,165 U_{min}=-7,211	U_{max}=5,263 U_{min}=5,079	U_{max}=1,201 U_{min}=1,125	U_{max}=24,166 U_{min}=22,791	U_{max}=21,123 U_{min}=19,924
20	U_{max}=13,158 U_{min}=12,702	U_{max}=-5,399 U_{min}=-5,499	U_{max}=6,971 U_{min}=6,786	U_{max}=2,960 U_{min}=2,879	U_{max}=25,839 U_{min}=24,376	U_{max}=22,47 U_{min}=21,278

Analyzing the numerical values of the calculated potentials, we can draw conclusions that confirm the additional rearrangement of the electron subsystem during film compression in comparison with the initial already polarized state. Namely: 1) the absolute values of the potentials of the external atomic layers of the film are large compared to the inside layers; 2) the potential values of the external layers increase with the level of film compression of 20 %, almost 2 times; 3) the levels of potential values on the inside layers, on the contrary, fell.

The tables 2, 3 and figures 6, 7 show the values of the forces, that act on a certain atom of film from the electronic, ionic subsystems and with a total account of influences, depending on the level of film compression.

Table 2. Projections of forces that act on a certain Hf atom of film from the electronic, ionic subsystems and with a total account of influences. The numbering of atoms, atomic layers correspond to the numbering in Fig. 5

% compressed		Layer 4 (inside)						Layer 1 (external)					
		atom 1 (Hf)			atom 5 (Hf)			atom 4 (Hf)			atom 7 (Hf)		
		F(x)	F(y)	F(z)	F(x)	F(y)	F(z)	F(x)	F(y)	F(z)	F(x)	F(y)	F(z)
0	el	0,242	-2,602	11,315	0,244	2,604	11,364	0,183	-0,086	0,353	0,181	0,076	0,351
	ion	-0,638	-0,436	4,030	-0,034	0,366	4,027	-0,082	-0,826	11,429	0,529	0,760	11,431
	sum	-0,396	-3,038	15,345	0,210	2,970	15,391	0,101	-0,911	11,782	0,710	0,836	11,783
5	el	2,626	-2,423	12,727	2,630	2,432	12,769	0,072	-0,125	0,135	0,068	0,119	0,133
	ion	-0,649	-0,458	4,729	-0,046	0,388	4,727	-0,068	-0,819	12,329	0,542	0,753	12,332
	sum	1,976	-2,881	17,456	2,584	2,820	17,495	0,004	-0,943	12,464	0,610	0,872	12,464
10	el	4,863	-2,610	11,215	4,875	2,626	11,282	-0,026	0,108	0,219	-0,027	-0,107	0,224
	ion	-0,666	-0,474	5,437	-0,063	0,405	5,434	-0,049	-0,804	13,222	0,559	0,739	13,224
	sum	4,197	-3,084	16,652	4,812	3,030	16,716	-0,075	-0,696	13,441	0,533	0,632	13,448
15	el	6,290	-3,124	15,278	6,281	3,147	15,337	-0,100	0,266	0,214	-0,093	-0,262	0,217
	ion	-0,688	-0,483	6,152	-0,086	0,414	6,150	-0,024	-0,781	14,104	0,583	0,716	14,106
	sum	5,602	-3,607	21,430	6,195	3,561	21,486	-0,124	-0,514	14,318	0,490	0,453	14,324
20	el	4,014	-4,583	16,001	4,023	4,613	16,081	-0,187	0,469	0,251	-0,182	-0,464	0,261
	ion	-0,717	-0,481	6,875	-0,116	0,413	6,873	0,008	-0,747	14,973	0,614	0,682	14,975
	sum	3,297	-5,064	22,876	3,907	5,026	22,953	-0,179	-0,278	15,224	0,433	0,218	15,236

Table 3. Projections of forces that act on a certain O atom of film from the electronic, ionic subsystems and with a total account of influences. The numbering of atoms, atomic layers correspond to the numbering in Fig. 5

% compressed		Layer 3 (inside)						Layer 2 (inside)					
		Atom 2 (O)			Atom 6 (O)			Atom 3(O)			Atom 8(O)		
		F(x)	F(y)	F(z)	F(x)	F(y)	F(z)	F(x)	F(y)	F(z)	F(x)	F(y)	F(z)
0	el	2,580	-5,540	24,631	2,587	5,551	24,762	-2,229	-3,305	1,881	-2,241	3,324	1,903
	ion	-0,156	-1,144	9,723	0,755	1,046	9,723	0,524	-0,536	12,453	-0,379	0,436	12,452
	sum	2,424	-6,684	34,354	3,342	6,596	34,485	-1,705	-3,842	14,333	-2,620	3,761	14,355
5	el	1,123	-1,839	13,261	1,126	1,823	13,327	-0,906	-3,126	1,269	-0,909	3,151	1,278
	ion	-0,168	-1,196	10,735	0,742	1,098	10,735	0,528	-0,556	13,604	-0,374	0,456	13,603
	sum	0,955	-3,035	23,996	1,868	2,921	24,061	-0,378	-3,682	14,872	-1,283	3,608	14,882
10	el	4,226	-5,561	9,741	4,247	5,552	9,799	0,264	-3,154	1,190	0,262	3,185	1,204
	ion	-0,182	-1,255	11,743	0,727	1,158	11,743	0,529	-0,576	14,771	-0,371	0,477	14,771
	sum	4,044	-6,816	21,485	4,974	6,710	21,542	0,793	-3,730	15,961	-0,108	3,662	15,975
15	el	2,449	-6,371	10,108	2,468	6,371	10,148	0,454	-1,840	2,437	0,455	1,861	2,471
	ion	-0,197	-1,324	12,749	0,710	1,227	12,749	0,528	-0,597	15,959	-0,371	0,499	15,959
	sum	2,252	-7,694	22,857	3,178	7,598	22,898	0,981	-2,438	18,396	0,085	2,360	18,429
20	el	5,063	-4,221	12,220	5,081	4,232	12,273	1,858	-2,659	2,519	1,877	2,681	2,553
	ion	-0,214	-1,402	13,752	0,692	1,305	13,752	0,521	-0,619	17,174	-0,376	0,521	17,173
	sum	4,849	-5,623	25,972	5,773	5,537	26,025	2,379	-3,279	19,692	1,500	3,202	19,726

% compressed		Layer 6 (external)						Layer 5 (external)					
		Atom 9 (O)			Atom 11 (O)			Atom 10 (O)			Atom 12 (O)		
		F(x)	F(y)	F(z)	F(x)	F(y)	F(z)	F(x)	F(y)	F(z)	F(x)	F(y)	F(z)
0	el	-1,903	-3,980	7,018	-1,895	3,973	7,029	1,196	-1,777	3,741	1,195	1,792	3,756
	ion	-0,520	-1,346	-2,484	0,384	1,243	-2,486	0,265	-0,270	-1,038	-0,631	0,172	-1,038
	sum	-2,423	-5,326	4,533	-1,511	5,215	4,543	1,461	-2,047	2,704	0,565	1,964	2,717
5	el	-1,690	-4,927	5,751	-1,690	4,923	5,769	2,111	-1,029	1,874	2,104	1,041	1,901
	ion	-0,502	-1,398	-1,923	0,401	1,296	-1,924	0,254	-0,273	-0,444	-0,641	0,176	-0,445
	sum	-2,192	-6,325	3,829	-1,289	6,219	3,844	2,365	-1,302	1,430	1,462	1,217	1,456
10	el	-0,902	-7,328	5,772	-0,909	7,319	5,788	0,472	-1,216	6,175	0,459	1,222	6,210
	ion	-0,484	-1,458	-1,355	0,419	1,356	-1,357	0,244	-0,278	0,145	-0,650	0,181	0,144
	sum	-1,386	-8,786	4,417	-0,490	8,675	4,431	0,716	-1,494	6,320	-0,191	1,403	6,355
15	el	0,078	-6,581	5,261	0,078	6,584	5,274	-0,885	-0,303	7,493	-0,901	0,311	7,530
	ion	-0,464	-1,527	-0,779	0,437	1,425	-0,781	0,238	-0,284	0,726	-0,655	0,188	0,725
	sum	-0,386	-8,108	4,482	0,516	8,009	4,494	-0,647	-0,587	8,219	-1,556	0,498	8,255
20	el	0,658	-5,972	1,208	0,661	5,975	1,221	-3,764	0,007	9,713	-3,781	0,005	9,743
	ion	-0,445	-1,605	-0,191	0,456	1,503	-0,193	0,238	-0,292	1,292	-0,655	0,196	1,292
	sum	0,213	-7,576	1,017	1,116	7,478	1,028	-3,526	-0,285	11,005	-4,435	0,201	11,035

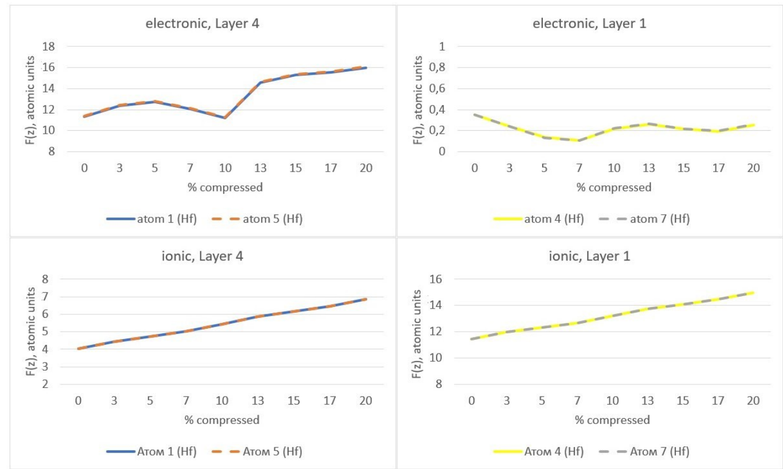

Fig. 6. Projections of forces that act on a certain Hf atom of film from the electronic, ionic subsystems

Analyzing the forces that act on an individual atom of the film from the electronic and ionic (core) subsystems of the rest of the film, we can draw the following conclusions:

1) the projections of forces on the direction 100 (on the z-axis of the Cartesian coordinate system, the direction along which the film was compressed) had the highest values, approximately an order of magnitude greater than the values of the projections on the X and Y axes;

2) the signs of the projections of forces on the z axis were the same for all atoms and all levels of compression, except for oxygen atoms from the external sublayer of the external layer;

3) the value of the projections of forces on the z axis, which originated from the classical ionic interaction, increased monotonically with increasing film compression level for all atoms. Whereas, the values of the projections of forces on the z axis, which came from the electron interaction, taking into account the quantum exchange-correlation interaction of electrons among themselves, behaved nonmonotonically with an increase in the level of film compression.

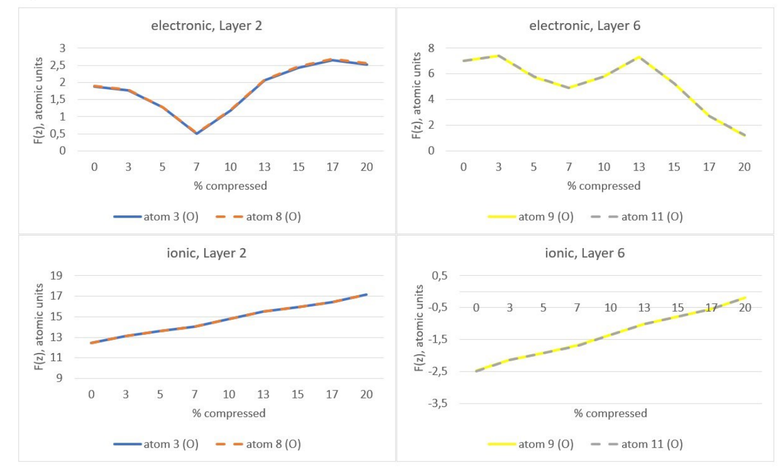

Fig. 7. Projections of forces that act on a certain O atom of film from the electronic, ionic subsystems

The study proved that compressing the film along the direction of polarization led to an increase in its polar distortion, but with a certain non-monotonic behavior.

Conclusion

The valence electron density spatial distribution, the Coulomb potentials, the forces that act on an individual atom from the electronic and ionic subsystems of infinite free-standing HfO_2 film and cluster under mechanical action were calculated in the framework of the density functional and *ab initio* pseudopotential theories.

The polarization charge distribution of valence electrons, which leads to piezoelectric effects, was observed in HfO_2 nanofilms, while in HfO_2 nanoclusters the charge distribution remained uniform both in the uncompressed and in the compressed state.

The compressing the HfO_2 film along the direction of polarization led to an increase in its polar distortion, but with a certain non-monotonic behavior.

References

1. *Liu J.; Zuo H., Xi, W., Luo Y., Yao D., Chen Y., Wang K., Li Q.* Wind Energy Harvesting Using Piezoelectric Macro Fiber Composites Based on Flutter Mode // Microelectron. Eng. - 2020, **-231.** - P.111333.
2. *Buragohain P., Lu H, Richter C., Schenk T., Kariuki P., Glinsek, Hiroshi Funakubo S., et al.* Quantification of the Electromechanical Measurements by Piezoresponse Force Microscopy // Adv. Mater. - 2022.**-34.**-P. 2206237.
3. *Dutta S, Buragohain P., Glinsek S., Richter C., Aramberri H., Lu H., Schroeder U., Defay E., Gruverman A., Íñiguez J.* Piezoelectricity in hafnia // Nature Communications.-2021.-**12**.-P.7301.
4. *Balabai R., Solomenko A., Radchenko T., Tatarenko V.* Functionalization of Quasi-Two-Dimensional Materials: Chemical and Strain-Induced Modifications // Progress in Physics of Metals. – 2022. - **23**. – P.147.
5. *Sang X., Grimley E.D., Schenk T., Schroeder U., Lebeau J.M.* On the structural origins of ferroelectricity in HfO2 thin films // Appl. Phys. Lett.-2015.-**106**.-P. 162905.